

## **Benefits of the S/F Cask Impact Limiter Weldment Imperfection**

**Jeong-Hoe Ku, Ju-Chan Lee, Jong-Hun Kim,  
Seong-Won Park, and Hyun-Soo Park**

Korea Atomic Energy Research Institute  
150 Dukjin-dong Yusong-gu, Taejeon 305-353, Korea

jhku@kaeri.re.kr

(Received November 7, 1999)

### **Abstract**

This paper describes the beneficial effect of weldment imperfection of the cask impact limiter, by applying intermittent-weld, for impact energy absorbing behavior. From the point of view of energy absorbing efficiency of an energy absorber, it is desirable to reduce the crush load resistance and increase the deformation of the energy absorber within certain limit. This paper presents the test results of intermittent-weldment and the analysis results of cask impacts and the discussions of the improvement of impact mitigating effect by the imperfect-weldment. The rupture of imperfect weldment of an impact limiter improves the energy-absorbing efficiency by reducing the crush load amplitude without loss of total energy absorption. The beneficial effect of weldment imperfection should be considered to the cask impact limiter design.

**Key Words** : intermittent-weld, weldment rupture, energy absorption, efficiency

### **1. Introduction**

In most transportable components, energy absorbers such as the cask impact limiter are commonly used to protect the components from the impact accident. The energy absorbing capability of an energy absorber is controlled by several factors such as mean crush load, maximum crush load, maximum crush distance, etc[1]. The energy absorber is designed to absorb the kinetic energy of the system by its irreversible plastic deformation. A spent nuclear fuel transportation

cask should maintain its structural integrity under the hypothetical 9 m free drop impact condition as described in IAEA regulations[2]. The safety of a cask against an impact accident is controlled by the structural stiffness of the cask body and the impact absorbing characteristics of the impact limiter.

In most case, the cask impact limiter consists of the metal jacket structure and the shock absorbing materials such as balsa wood, redwood, and polyurethane foam, since the foam filled metal structure shows good energy absorbing

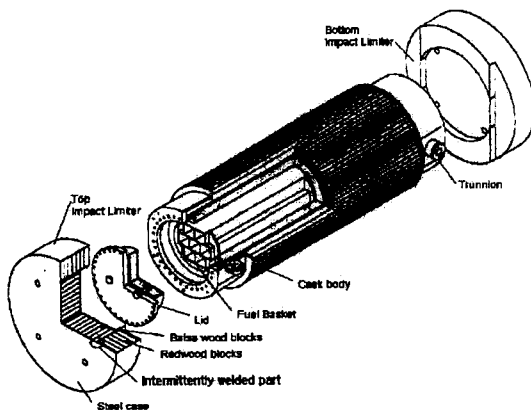
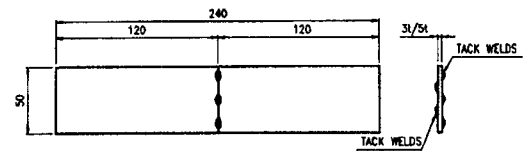
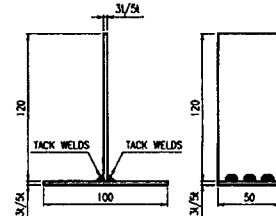


**Fig. 1. Schematic Drawings of a Typical PWR Spent Fuel Transport Cask**

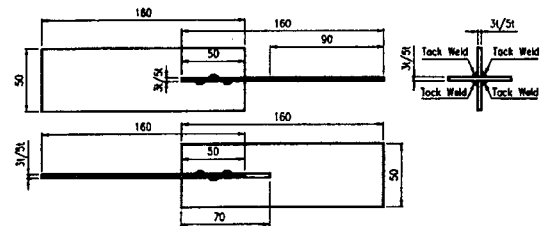
performance[3-6]. Also, in cask impact limiter fabrication, intermittent welds are practicably inevitable in some inner joints between the case and gusset plates to avoid the welding distortion and the combustion of wood or foam fillers during the welding process. These weldments have lower strength than the plate or fully welded joints, and therefore, some of these are ruptured during impact-deformation. However, until recently, the energy absorbing effect by the metal structure and the interaction of the metal structure with filler materials was neglected in most cask impact analyses[7,8]. And most studies on the thin-walled metal structure considered seamless or fully welded tubes, and assumed that weldment has strength equivalent to the tube wall. In this study, the characteristics of the intermittent weldment of the cask impact limiter were analyzed by the test of intermittently welded specimens, and the influence of weldment rupture on the cask impact absorbing behavior was evaluated by finite element analysis. In this study, it was assumed that the cask impact limiter consisted of stainless steel metal structure of 5 mm thickness and balsa wood and redwood for energy absorbing materials.



(a) I-shape tensile test specimen



(b) T-shape combined shear test specimen



(c) X-shape pure shear test specimen

**Fig. 2. Test Specimens of Intermittent-weld Joint**

## 2. Intermittent Welded Joint Strength Evaluation

### 2.1. Test Specimens and Methods

The material test specimens were prepared to obtain the material characteristics of the cask impact limiter materials. Since the stainless steel sheet with a thickness of 5 mm was used for the casing material, sheet type standard tensile test specimens were prepared and tested according to the ASTM E8M standards[9]. The size of the specimens had a overall length of 200 mm, width of 12.5 mm and thickness of 5 mm. Balsa wood and redwood specimens were prepared, and tested according to the ASTM D143 standards[10] to gain the compressive stress-strain behaviors for

each grain direction.

A series of tensile, shear and combined shear test specimens were prepared and tested on the intermittent-weld joints according to the ASTM E8 standards to evaluate the joint strength of intermittent-weldment of the cask impact limiter. Fig. 2 shows the shapes and dimensions of intermittent-weld specimens. The weld specimens consisted of three groups, tensile, pure shear and combined shear specimens, each with the same width of 50 mm. All specimens were made from 304 stainless steel plates, which are commonly used in the cask impact limiter case, with thickness of 5 mm. The welding condition was conformed to the condition of the impact limiter case as close as possible. All specimens had intermittent weldments for both sides at the contacted joint between two plates in asymmetric positions to minimize the mutual heat affection between the weldments, with 4 to 8 total weld points for each specimen group. Tensile specimens were made from two same plates with a butt joint, and combined shear specimens were made from two plates with different lengths, which were connected into a T-shape with two fillet joints. In pure shear specimens, two plates were crossed over a 60 mm length by making a long slot on one side of the plate, so they had four fillet joints. To raise the confidence of the tests, each specimen group consisted of three sets. In the combined shear test, a specially devised jig was used to fix the base plate of the T-shape specimen.

The tests were conducted by the displacement control method using an Instron 1332 universal testing machine at room temperature at a cross-head speed of 2 mm/min. Because of the high ductility of stainless steel, a wedge grip was used. Since measuring the strain of the weldment is impossible, the strain of a plate at a location more than 50 mm from the weldment was measured by

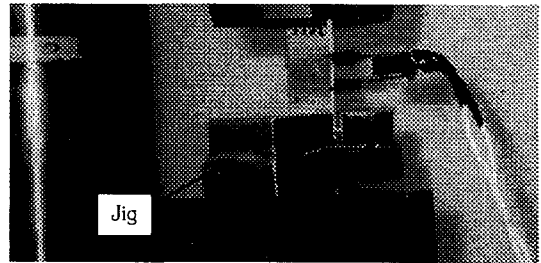


**Fig. 3. Shear Test of a T-shape Specimen**

the LVDT until weldment ruptured, and the maximum load that a welded specimen can sustain before its failure was obtained. Fig. 3 shows the test of T-shape combined shear specimen. The objective of this test was to obtain the maximum force of the intermittently welded weldment per unit weld, and to find the failure behavior of the intermittently welded joints under each loading mode.

## 2.2. Test Results and Discussions

From the tensile test with standard specimens, the yield strength and ultimate strength of 304 stainless steel were obtained as 241 MPa and 600 MPa respectively. The tensile specimens were ruptured at a strain about of 0.5, which means that stainless steel is very ductile. The crush strengthes and lock-up strains of balsa wood were 12.2 MPa and 0.76 respectively for parallel to the grain direction and 1.7 MPa and 0.67 respectively for perpendicular to the grain direction. The crush strengthes and lock-up strains of redwood were 30.7 MPa and 0.62 respectively for parallel to the grain direction and 7.8 MPa and 0.61 respectively for perpendicular to the grain direction.

The test results for intermittent-weld specimens are presented in Table 1. In Table 1, the first character represents the load mode, T for tensile, S for combined shear and X for pure shear, the second is the plate thickness, the third is the

**Table. 1. Test Results of Intermittent-weld Specimens**

Load type	Specimen	$\sigma_{\max}$ at plate (MPa)	$P_{\max}$ (kN)	$P_{\max} /$ Weld (kN)	$P_{\max(\text{ave})} /$ Weld (kN)	Number of weld (ea)
Tensile	T541	215	54.30	13.58	14.15	4
	T542	234	59.73	14.93		
	T543	223	55.81	13.95		
	T551	247	62.33	12.47	12.86	5
	T552	249	63.17	12.63		
	T553	263	67.39	13.48		
	T561	275	69.83	11.64	11.42	6
	T562	264	66.92	11.15		
	T563	272	68.73	11.46		
Combined shear	S541	137	34.96	8.74	9.01	4
	S542	142	37.02	9.26		
	S543	140	36.12	9.03		
	S551	188	48.18	9.64	9.62	5
	S552	184	47.26	9.45		
	S553	190	48.79	9.76		
	S561	220	56.52	9.42	9.21	6
	S562	208	53.89	8.98		
	S563	215	55.45	9.24		
Pure shear	X541	131	32.26	8.07	6.81	4
	X542	97	24.13	6.03		
	X543	101	25.30	6.33		
	X561	188	46.90	7.82	7.18	6
	X562	171	42.70	7.12		
	X563	159	39.67	6.61		
	X581	251	62.81	7.85	7.95	8
	X582	246	61.39	7.67		
	X583	267	66.66			

number of weld points, and the fourth is the serial number. In tensile tests, though some weldments failed, the remaining weldments were extended about 1 mm until the final rupture, and the failure happened slowly, showing a ductile failure. In combined and pure shear tests, however, the specimens were fractured abruptly, showing a

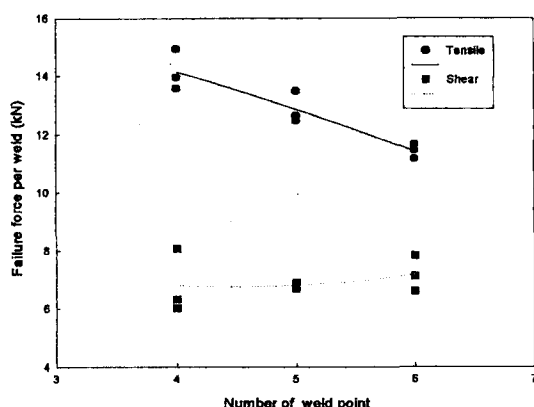
brittle failure, though the stresses of plates were not reached at their yield stress.

Fig. 4 shows the variation of the failure forces of intermittent-weld for tensile and shear modes. For the tensile specimens, the ruptured surface of the weldment had a semi-ellipsoidal cross section with a length of 6~9 mm and a width of about 2.1~

**Table 2. Summary of Test Results of Intermittent-weld Specimens**

Number of welds (ea)	Tension mode			Shear mode		
	$\sigma_{\max}$ at plate (MPa)	$\sigma_{\max}$ at weld (MPa)	Sn (kN) (MPa)	$\sigma_{\max}$ at plate (MPa)	$\tau_{\max}$ at weld	Ss (kN)
4	224	911	14.15	110	469	6.81
5	253	828	12.86	132	469	6.80
6	270	735	11.42	173	495	7.18

\* Sn, Ss : Maximum tensile and shear force per weld

**Fig. 4. Variation of the Failure Forces of Intermittent-weld**

2.4 mm. The failure force for tensile mode is reduced with the increase of the welding points. The cross sectional area was about 15.5 mm<sup>2</sup>. However, for combined shear and pure shear specimens, the cross sectional areas was 14.5 mm<sup>2</sup>, and the failure force was slightly increase with the increase of the welding points.

As shown in Table 1 and Fig. 4, the tensile specimens can sustain a higher load than the shear specimens. Most shear specimens were ruptured before the stress of the plate had reached the yield stress, however, most tensile specimens were ruptured when the stress of the plate exceeded the yield stress. This fact means that the

weldment can share the strength with the plates until a certain level. Table 2 presents the summarized data of the test results for the maximum tensile and shear force per weldment. Since the pure shear specimens have even numbers of welding points, the shear force values for 5 welding points were derived from the results of the combined shear specimens. However, as the combined shear specimen does not represent the pure shear mode, the stress evaluation was carried out to classify the shear component from the force equilibrium condition. From the test results, it was shown that the intermittent-weld joint failed without rupture of the plate regardless of the loading mode because of its weaker strength than that of the plate, and the stress concentration at the weldments.

### 2.3. Benchmark Analysis of Weldment Rupture

A benchmark analysis was carried out on the T-shape combined shear specimen with 4 welding points. The primary objective of this analysis is to check the capability and precision of LS-DYNA[11] code for the simulation of the failure analysis of the intermittent-weld joint by comparing the analysis results with the test results. This analysis requires the capability of code for

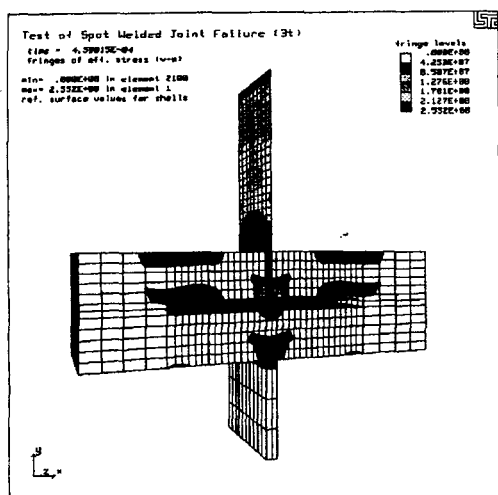


Fig. 5. Weldment Rupture Analysis Model of a T-shape Specimen

intermittent-welded to surface interface element with failure criteria with other common contact capabilities. LS-DYNA assumes that failure of the tack-welded joints occurs when:

$$\left(\frac{f_n}{S_n}\right)^n + \left(\frac{f_s}{S_s}\right)^m \geq 1$$

where  $S_n$  and  $S_s$  represent the normal and shear forces at failure, and  $f_n$  and  $f_s$  are the normal and shear interface forces, respectively. Component  $f_n$  is nonzero for tensile values only. For tie-breaking interfaces, the above failure criterion is used with  $m=n=2$ . Because the purpose of this analysis is to compare with the test data, the boundary conditions and load conditions were applied as similar as possible with the test condition. Fig. 5 shows the analysis model and stress contours of the specimen. Fig. 6 shows the resultant force-displacement curve of the T-shape specimen model. The analysis result showed good agreement with the test result. According to the test result, as presented in Table 1, the maximum load which can be received by the T-shape

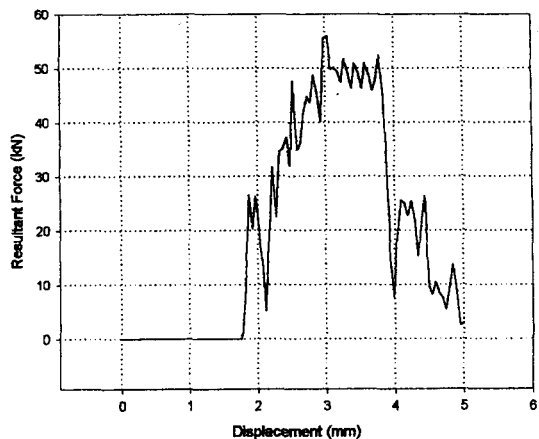


Fig. 6. Resultant Force-displacement History for Intermittent-weld Joint of T-shape Specimen

specimen with 4 weld points is 56.6 kN, and the analysis result was 55.9 kN, which was very close to the test result. Therefore, the capability of LS-DYNA code to simulate the failure analysis of intermittent-weld joint was verified.

### 3. Improvement of Impact Mitigating by the Weldment Rupture

To evaluate the effect of the weldment rupture on the cask impact absorbing behavior, a series of impact analyses were carried out by the analytical method. A typical spent PWR fuel transport cask, as shown in Fig. 1, was considered in this analysis. The outer diameter of the cask body is 1.6 m, the total length is 5.3 m, and the total loaded weight of cask is about 70 tons. The impact limiters were constructed from stainless steel casing and wood blocks. The steel casing has 8 gusset plates in the radial direction which enclose the wood blocks. Balsa wood and redwood were used as energy absorbing materials. Three impact orientations were considered in this evaluation for vertical, horizontal and corner drops, because the regulation requires the evaluation for the direction

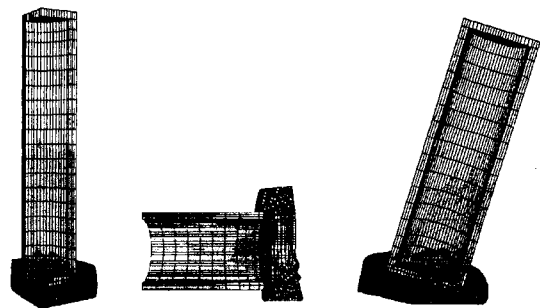
**Table 3. Comparison of Analysis Results According to the Welding Condition for Each Drop**

	Item	Case (a)	Case (b)	Comparison of Case(b) with (a)
Vertical Drop	Max. displacement (cm)	13.1	14.3	9% increased
	Max. impact force (MN)	79.4	72.7	8% decreased
	Max. acceleration (g)	87.5	78.3	11% decreased
Horizontal Drop	Max. displacement (cm)	22.8	25.5	12% increased
	Max. impact force (MN)	52.8	39.6	25% decreased
	Max. acceleration (g)	71.7	53.6	25% decreased
Corner Drop	Max. displacement (cm)	40.8	42.3	4% increased
	Max. impact force (MN)	46.8	46.5	Similar
	Max. acceleration (g)	64.8	64.6	Similar

in which the maximum damage is expected. For each impact orientation, two weld conditions, full weld and intermittent weld, were evaluated to assess the effect of the weld condition on the cask impact behavior. In this study, only the global behaviors of the cask drop impact were considered, and the local damage of the cask was neglected. Therefore, the degree of cask damage was evaluated based on the magnitude of the impact force, which acts on the unyielding target surface.

### 3.1. Analysis Model

The structural analysis was conducted by three dimensional analysis models using the LS-DYNA3D code. Quarter-sections of the cask were modeled for vertical and horizontal drop impacts and a half section was modeled for corner drop impact using the geometric symmetries, and the symmetry boundary conditions were applied to all nodes located on the symmetry planes. The cask body was modeled as a simplified hollow cylinder

**Fig. 7. Deformed Shapes of Cask Under 9m Free Drop Impact**

with equivalent mass to the cask weight.

The metal structure of the steel case and gusset plates and their interfaces with wood blocks were taken into account as accurately as possible, because balsa wood and redwood blocks were inserted into the steel case in axial and radial directions, and had orthogonal crush characteristics. Accordingly, the interfaces between the wood blocks and the steel case were considered by the automatic single surface contact

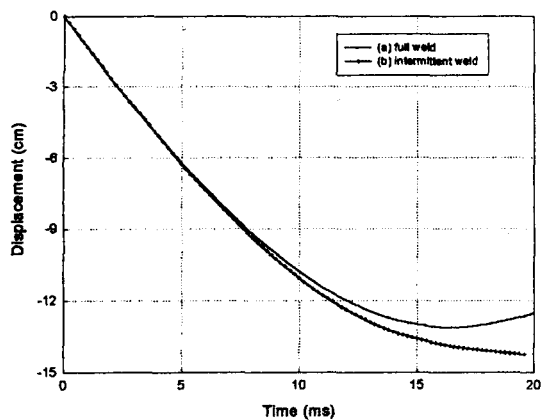


**Fig. 8. Comparison of Displacement-Time Histories According to the Weld Condition of Impact-limiter Under Vertical Drop Impact**

element, and the orthogonal crush characteristics of woods according to the grain directions which were obtained from the crush test were applied. The material properties were assumed as elastic-plastic with strain hardening. The initial velocity of 13.3 m/s was applied to all nodes as a load condition for all impact conditions. The target surface was simulated by the stone wall option as an infinite flat rigid surface fixed in the space.

The intermittent-welded part of the impact limiter was simulated using the node to intermittent-welded contact option with the strength of the intermittent-weld joint obtained from the test. Impact limiter models consisted of following two cases:

- Case-(a) : full weld in all weldment
- Case-(b) : intermittent-weld between gusset plates and outer case

The Case-(b) model consisted of 13,316 nodes, 9,344 solid elements and 1,504 shell elements. The intermittent weldment was simulated by 32 node to welded interface elements for radial

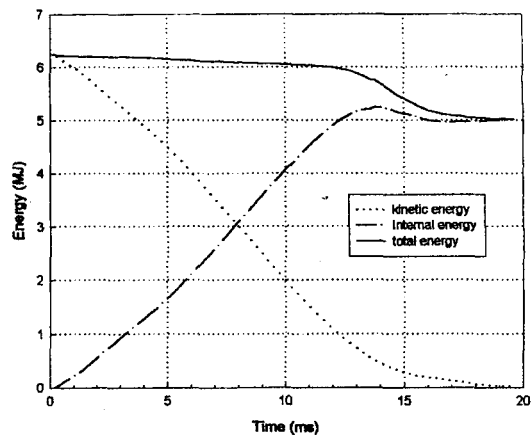


**Fig. 9. Energy-time Histories of the Intermittent-weld Cask Under Vertical Drop Impact**

direction of 180 degree for each impact limiter with a strength of  $S_n$  as 11.42 kN and  $S_s$  as 7.18 kN.

### 3.2. Analysis Results

If the cask is impacted onto the unyielding target from a 9 m free fall, the kinetic energy of the cask is transformed into strain energy by the plastic deformation of the impact limiter. The cask impact analysis results for each drop impact are presented in Table 3. Fig. 7 shows the deformed shapes and stress contours of the cask for three impact orientations. In Fig. 7, it was assumed that the all welded joints of the impact limiter cases were fully welded. Like most foam-filled tube type energy absorbers, the cask impact limiter also absorbed the impact energy by the plastic deformation of the steel case and the cellular filler material.

Fig. 8 shows the comparison of displacement-time histories for the two different weld conditions of the impact limiter for vertical drop impact. For vertical drop impact, as shown in Fig. 8 and Table



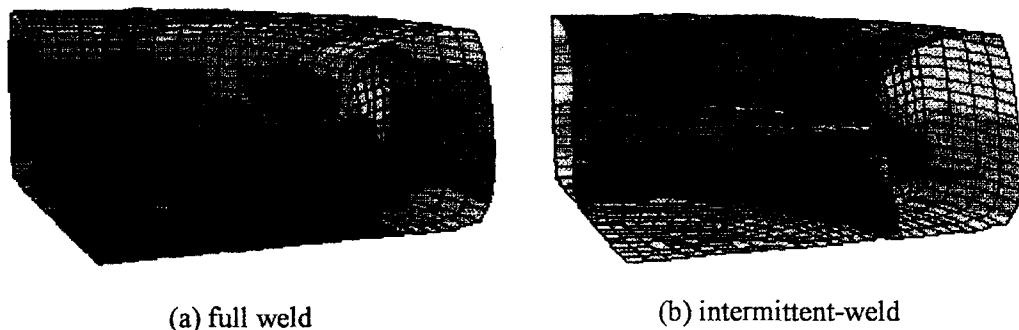


**Fig. 10. Comparison of Stress Contour of Impact Limiter Case Under Vertical Drop Impact**

3, the displacements of the intermittent-welded impact limiter was larger than that of the fully welded impact limiter. Since the cask body was assumed as elastic, the maximum deflections represent the maximum deformations of the impact limiters. The maximum deformation of the Case-(b) model was 14.3 cm, which was 10% more than the maximum deformation of 13.1 cm of the fully welded model of Case-(a). This means that the intermittent-welded impact limiter was deformed more because some of the intermittent-welded joints were ruptured. Fig. 9 shows the energy-time histories for the intermittent-welded impact limiter under vertical drop impact. The kinetic energy due to the free fall of the cask is transformed into strain energy by the deformation of the impact limiter during the impact-deformation. The strain energy is transformed again into kinetic energy when the cask rebounds. However, if a large deformation occurs, the energy loss will increase[12]. As shown in Fig. 9, the total energy of the system for the intermittent-welded impact limiter decreased at 12 ms after the impact initiation. It was interpreted that this energy dissipation was due to weldment rupture during the deformation of the impact limiter. The stress contours of the impact limiter steel case are compared for fully and intermittent-welded impact limiters in Fig. 10. As seen in Fig. 10, the stress concentrations of the intermittent-welded impact

limiters were much less than those of the fully welded impact limiter, because if some of the welded joints of the steel jacket are ruptured, the steel jacket no longer constrains the deformation of wood blocks and cause the steel jacket to lose its constraining effect on the wood blocks. Fig. 11 shows the comparison of impact force-time histories for vertical drop impact for two different weld conditions. The sudden increase and decrease of impact forces for both cases at the beginning of the impact means that the steel jacket of the impact limiter has a large compression resistance until it buckles if the impact limiter is impacted on the bottom surface at the same time. The maximum impact force decreased 8%. Also, as presented in Table 3, the maximum deformations of the impact limiter increased 9%, and the maximum accelerations of the cask body decreased 11% according to the variation of the weld condition of impact limiter. Fig. 12 shows the comparison of displacement-time histories for horizontal drop impact. For horizontal drop impact, as shown in Fig. 12 and Table 3, the displacements of the intermittent-welded impact limiter was 12% more than fully welded impact limiter. As shown in Fig. 13, the intermittent-welded impact limiter crushed out more than the fully welded impact limiter, and therefore the stress concentrations at the welded joints were much reduced. Fig. 14 shows the

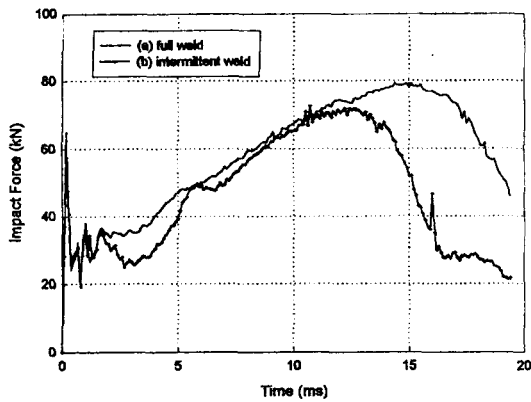


**Fig. 11. Comparison of Impact Force-time Histories According to the Weld Condition of Impact Limiter Under Vertical Drop Impact**

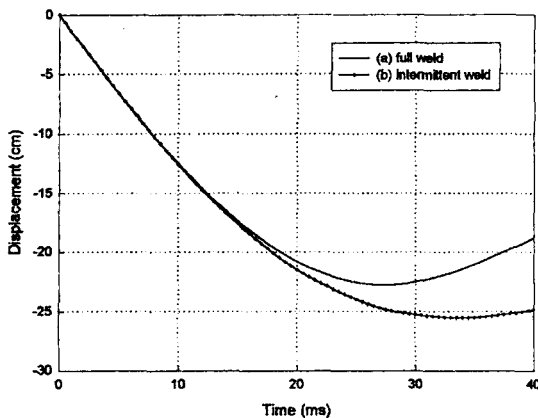
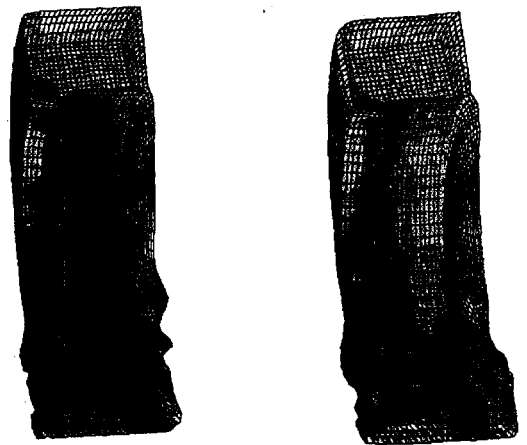


**Fig. 12. Comparison of Displacement-time Histories According to the Weld Condition of Impact-Limiter Under Horizontal Drop Impact**

impact force-time histories for horizontal drop impact. As presented in Table 3, the maximum impact force decreased 25%, and the maximum acceleration of the cask body decreased 25% for the intermittent-welded impact limiter.

However in corner drop impact, as shown in Fig. 15 and 16, the displacement and impact force-time histories were very similar for both weld conditions. The maximum deformation increased



(a) full weld

(b) intermittent-weld

**Fig. 13. Comparison of Stress Contour of Impact Limiter Case Under Horizontal Drop Impact**

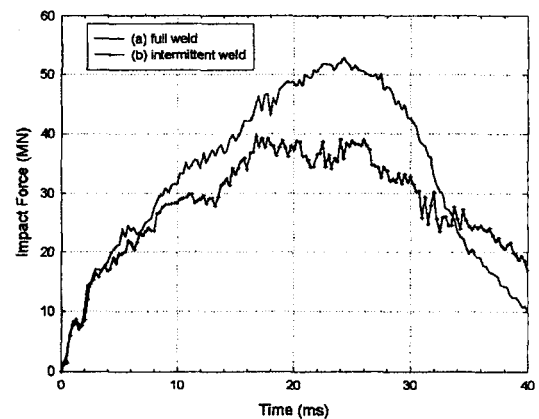


**Fig. 14. Comparison of Impact Force-time Histories According to the Weld Condition of Impact Limiter Under Horizontal Drop Impact**

only 3% in the intermittent-welded impact limiter, and the maximum impact force and acceleration were similar. The impact behavior in corner drop impact seemed not to be affected by the weld condition.

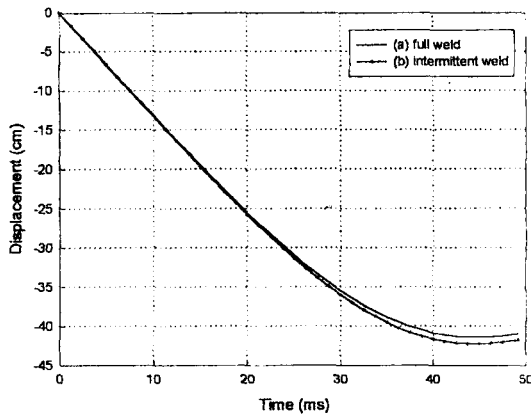


**Fig. 15. Comparison of Displacement-time Histories According to the Weld Condition of Impact Limiter Under Horizontal Drop Impact**

#### 4. Discussions

The steel jacket of the impact limiter protects the shock absorbing filler materials and maintains its structural strength for handling in normal operation. It also absorbs impact energy by the buckling deformation with the deformation of shock absorbing material in the impact accident. Consequently, since the steel jacket plays the opposite roles of absorbing the impact and hindering the deformation of the shock absorbing material, the stiffness of the steel jacket has a significant effect on the impact absorbing behavior of the cask. Also, the strength of weldment controls the boundary conditions on the deformation of the steel jacket and changes the deformation constraining conditions of the shock absorbing material, and thus changes the mean crush strength of the impact limiter.

As shown in Fig. 10a and Fig. 13a, high stresses are concentrated at the welded joints of the steel jacket because the steel case confines the deformation of the wood blocks filled into the steel jacket, and the welded joints also confine the buckling deformation of the steel jacket itself. The

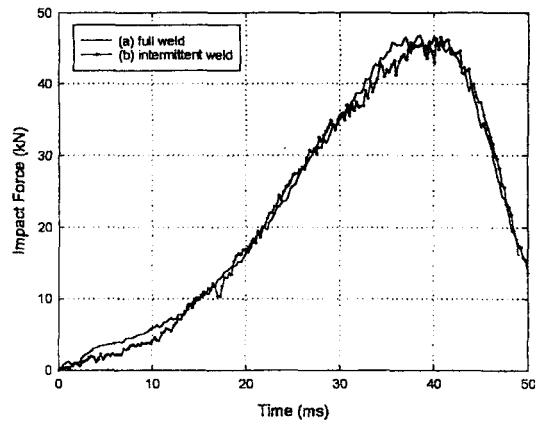


**Fig. 16. Comparison of Impact Force-time Histories According to the Weld Condition of Impact Limiter Under Horizontal Drop Impact**

compressed wood blocks in the steel jacket act as internal pressure on the enclosing steel jacket. However, if some welded joints which receive high stress are ruptured, the steel jacket loses the confining role for wood blocks, and the boundary condition of shell buckling is also changed. As discussed by many researchers, the buckling strength of a thin walled structure is very sensitive to the edge boundary condition[13,14].

If some of the weldments are intermittent-welded and thus have a lower strength, the weldment will maintain its confining effect for wood blocks at first, until the stress of the steel jacket plate reaches at a certain plastic region, and then will be eventually ruptured when the stress reaches its failure force. Therefore, the weldment rupture will increase the total deformation of the impact limiter by losing the wood confining effect, and decrease the crush strength of the steel jacket by changing the edge boundary condition. As shown in Fig. 10b and Fig. 13b, high stress concentrations at the welded joints of the steel jacket are significantly mitigated if some weldments of the steel case are ruptured in a later part of the impact duration.

As discussed above, the application of intermittent weld onto some weld joints of the impact limiter has several advantages besides the improvement of impact mitigation capability without diminishing the thermal shielding protecting role since the intermittent weld is applied only to the inner joints of the steel case. It can reduce the manufacturing time for the impact limiter and materials needed for welding, since the total welding work is reduced. The important advantage is that combustion of the wood blocks from welding heat can be prevented because intermittent weld generates much less heat and welding deformation. In the application of intermittent welds in the impact limiter, the proper location and strength of weldment should be considered.

## 5. Conclusions

The steel jacket of the cask impact limiter has several functions such as protecting the filler materials which inserted in it for both the shock absorption and thermal shielding, and also maintaining the structural strength for handling in normal operation. Of these functions, it should be noted that it also engages in impact energy absorption by its buckling deformation with the deformation of filler material in the impact accident.

If an intermittent-weld, which has a lower strength and ruptures during the impact deformation process, is applied properly onto a cask impact limiter, the impact mitigating function of the impact limiter can be much improved. Since the constraining effect of the weldment for energy absorbing filler materials is changed, the cask impact behavior is also changed by the weldment rupture during the deformation of the impact limiter.

Proper selection of the location and the proper

strength of the intermittent welds can effectively mitigate the maximum impact force which occurs at the later part of the impact by playing both the constraining and the suitable release for the deformation of filler materials and its buckling deformation. The application of intermittent welds to the impact limiter case has several more benefits besides the improvement of the impact mitigation effect than the fully welded for the same impact limiter, such as reducing welding distortion of the metal jacket in the fabrication process, and reducing fabrication cost without any loss of its functions.

## Acknowledgement

This work has been carried out under the Long-and-Mid-term Nuclear R&D Program supported by MOST.

## References

1. N. Jones and T. Weirzbicki, "Structural Crashworthiness," pp. 96-117, Butterworths, London, (1983).
2. IAEA Safety Standards No. ST-1, Regulations for the Safe Transport of Radioactive Materials, (1996).
3. W. Johnson and S. R. Reid, Metallic Energy Dissipating Systems, Applied Mechanics Reviews, Vol. 31, No. 3, (1978).
4. B. E. Lampinen and R. A. Jeryan, Effectiveness of Polyurethane Foam in Energy Absorbing Structures, Trans. SAE 91, pp.2059-2076, (1982).
5. W. Abramowicz and T. Weirzbicki, "Axial Crushing of Foam-Filled Columns," Int. J. of Mech. Sci, Vol. 30, No. 3, pp. 263-271, (1988).
6. K. R. F. Andrews, G. L. England and E. Ghani, Classification of the Axial Collapse of

- Cylindrical Tubes Under Quasi-Static Loading, *Int. J. of Mechanical Science*, Vol.25, No.9-10, pp. 687-696, (1983).
7. F. P. Henry and C. W. Williams, Rigid Polyurethane Foam for Impact and Thermal Protection, PATRAM95, pp.1161-1168, (1995).
  8. G. W. Wellman, Transportation System Impact Limiter Design using Rigid Polyurethane Foam, SAND84-2271 DE85 015088, Sandia National Laboratories, (1984).
  9. ASTM Standards Vol. 03.01 Metals-Mechanical Testing, E8M, Standard Methods for Tension Testing of Metallic Materials [METRIC], pp. 146-169, (1986).
  10. ASTM Standards Vol. 04.09 Wood, D143-83, Standard Methods of Testing of Small Clear Specimens of Timber, pp. 48-104, (1987).
  11. J. O. Hallquist, LS-DYNA3D Theoretical Manual, Version 950, Livermore Software Technology Corporation, (1999).
  12. Z. H. Zhong, Finite Element Procedures for Contact-Impact Problems, Oxford, pp. 136-167, (1993).
  13. B. G. Johnston, Guide to Stability Design Criteria for Metal Structures, Structural Stability Research Council, John Wiley and Sons Inc., 3rd ed., (1976).
  14. S. P. Timoshenko and J. M. Gere, Theory of Elastic Stability, 2nd ed., 1961.